Journal of Cellular Biochemistry 93:1282–1296 (2004)

c-Myc Localization Within the Nucleus: Evidence for Association With the PML Nuclear Body

Kelly P. Smith,[1]* Meg Byron,[1] Brenda C. O'Connell,[2] Rose Tam,[1] Christoph Schorl,[2] Isil Guney,[2] Lisa L. Hall,[1] Pooja Agrawal,[2] John M. Sedivy,[2] and Jeanne B. Lawrence[1]

[1]Department of Cell Biology, University of Massachusetts Medical School, 55 Lake Avenue North, Worcester, Massachusetts 01655
[2]Department of Molecular Biology, Cell Biology and Biochemistry, Brown University, Providence, Rhode Island 02912

Abstract Definitive localization of c-Myc within the nucleus is important to fully understand the regulation and function of this oncoprotein. Studies of c-Myc distribution, however, have produced conflicting results. To overcome technical challenges inherent in c-Myc cytology, we use here three methods to visualize c-Myc and in addition examine the impact of proteasome inhibition. EYFP or HA-tagged Myc was reintroduced by stable transfection into *myc* null diploid rat fibroblasts, replacing endogenous Myc with tagged Myc expressed at or near normal levels. This tagged Myc is shown to functionally replace the endogenous Myc by restoration of normal cell morphology and growth rate. We were able to confirm key findings using antibodies to the endogenous c-Myc and/or its partner, Max. Contrary to some published reports, by all three methods the c-Myc protein in rat fibroblasts distributes predominantly throughout the nucleus in a dispersed granular pattern, avoiding the nucleolus. Importantly, however, several findings provide evidence for an unanticipated relationship between c-Myc and PML nuclear bodies, which is enhanced under conditions of proteasome inhibition. Evidence of Max concentration within PML bodies is shown both with and without proteasome inhibition, strengthening the relationship between PML bodies and Myc/Max. Some accumulation of Myc and Max in nucleoli upon proteasome inhibition is also observed, although co-localization of ubiquitin was only seen with PML bodies. This work provides a comprehensive study of c-Myc distribution and also presents the first evidence of a relationship between turnover of this oncoprotein and PML nuclear bodies, known to break down in certain cancers. J. Cell. Biochem. 93: 1282–1296, 2004.

Key words: c-Myc; PML; Max; nucleus; proteasomes

Deregulation of the c-*myc* proto-oncogene is believed to causally contribute to the genesis of up to 30% of all human cancers [Henriksson and Luscher, 1996]. The c-Myc protein has been implicated in the regulation of transcription, but its physiological function as well as its biochemical mode of action remains poorly defined [Claassen and Hann, 1999; Cole and McMahon, 1999; Amati et al., 2001]. Myc requires association with a partner protein called Max in order to bind DNA and influence transcription [Kretzner et al., 1992]. Myc and Max can alternatively associate with a number of other proteins in a complex network of interactions [Baudino and Cleveland, 2001]. A better understanding of the role of c-Myc in cell growth and proliferation would be aided by determining the in vivo behavior of the protein within the complex structure of the cell.

Early studies reported that Myc is located predominantly in the nucleus [Abrams et al.,

Grant sponsor: NIH Public Health Service (to JMS); Grant number: R01 GM-41690; Grant sponsor: NIH Public Health Service (to JBL); Grant numbers: R01 GM-49254, R01 GM-68138; Grant sponsor: NIH (Predoctoral Training Grant to BOC); Grant number: GM-07601; Grant sponsor: NIH; Grant number: RR-15578.

*Correspondence to: Kelly P. Smith, Department of Cell Biology, University of Massachusetts Medical School, 55 Lake Avenue North, Worcester, Massachusetts 01655.
E-mail: Kelly.smith@umassmed.edu

Received 6 April 2004; Accepted 6 July 2004
DOI 10.1002/jcb.20273

1982; Hann et al., 1983]. It is increasingly appreciated that the nucleus contains a number of distinct, non-membrane bounded compartments such as SC35 domains, Cajal bodies and PML bodies, in which different sets of macromolecules concentrate, presumably for a common function [Lamond and Earnshaw, 1998; Shopland and Lawrence, 2000]. SC35 domains (the 10–30 prominent snRNP speckles) are enriched in a host of factors involved in pre-mRNA production [Moen et al., 1995], whereas Cajal Bodies have factors involved in metabolism of pre-mRNAs, nucleolar RNAs [Gall, 2000] and snRNAs [Darzacq et al., 2002]. PML (*prom*yelocytic *l*eukemia) nuclear bodies also referred to as PODs (PML oncogenic domains) [Dyck et al., 1994; Weis et al., 1994] and originally identified as ND10 (nuclear dot 10) [Ascoli and Maul, 1991], have generated much interest because of their intriguing connection to cancer. PML bodies are disrupted in acute promyelocytic leukemia (APL) due to a translocation that fuses the PML protein, a key factor in PML body formation, with the retinoic acid receptor protein. PML bodies contain multiple proteins, such as the transcription regulator protein Daxx, as well as numerous other factors involved in gene regulation, growth control, protein degradation, and apoptosis [reviewed in Zhong et al., 2000; Salomoni and Pandolfi, 2002].

Myc is a short-lived protein, with a half-life of approximately 30 min [Ramsay et al., 1986]. Myc protein levels are regulated by the ubiquitin-proteasome pathway [Gross-Mesilaty et al., 1998; Salghetti et al., 1999; Sears et al., 1999], which is a primary means for degradation of short-lived regulatory proteins [Hershko and Ciechanover, 1998]. The finding of ubiquitin [Everett, 2000], ubiquitin-dependent hydrolase (HAUSP) [Everett et al., 1997] and components of the proteasome [Fabunmi et al., 2001; Lallemand-Breitenbach et al., 2001; Wojcik and DeMartino, 2003] in the PML nuclear body has suggested that the PML body may be involved in proteasome-mediated protein degradation.

Given our increasing understanding of nuclear compartments, high-resolution localization of c-Myc within the nucleus could provide important new insights into its function. Cytological analysis of c-Myc has long been seriously hampered by its very low expression in normal cells, estimated to be as low as 1,000–3,000 molecules per cell [Waters et al., 1991], and the relatively low affinity and insensitivity of available antibodies. Thus, studies on Myc localization using antibodies against endogenous c-Myc or transient expression of exogenous, tagged Myc have produced conflicting results [Hann et al., 1983; Spector et al., 1987] (see Discussion). Evidence suggests that in the native state within nuclear structure c-Myc protein antigenic epitopes are masked, because the same epitopes can be highly antigenic when attached to another protein. More recently, GFP tagged Myc has been used to study c-Myc distribution, but these studies have also produced inconsistent results. In a transient transfection system, Yin et al. [2001] reported that GFP-Myc shows a marked localization in a "speckled" nuclear pattern that does not coincide with splicing factor domains. Contrary to this, during the course of our study a paper was published reporting that Myc was normally found dispersed throughout the nucleoplasm, again using GFP-Myc in transient transfections [Arabi et al., 2003].

In this study, we have used several approaches to investigate the in vivo distribution of c-Myc carrying different tags in stably transfected cell lines, in addition to investigations of the endogenous protein using two different anti-c-Myc antibodies. To achieve a more definitive study of c-Myc nuclear localization, we engineered cells to stably express two different epitope-tagged c-*myc* transgenes in a c-*myc* null rat fibroblast cell line that had previously been constructed by gene targeting [Mateyak et al., 1997]. Importantly, we demonstrate that the epitope-tagged Myc protein is fully functional because it complements all c-Myc−/− phenotypes at levels of expression equivalent or close to c-Myc levels found in normal cells. In cells expressing either EYFP (enhanced yellow fluorescent protein)-Myc or HA (influenza hemagglutin)-Myc, Myc was found in a dispersed granular nucleoplasmic pattern. Two anti-Myc antibodies produced a similar pattern in these cell lines. In addition, however, c-Myc was found to accumulate with Max in Daxx defined PML bodies and/or in the nucleolus in cells treated with the proteasome inhibitor MG132. Upon transient transfection of HeLa cells, Myc was found to accumulate with PML nuclear bodies without proteasome inhibition. We also present evidence for Max association with PML bodies in uninhibited cells.

MATERIALS AND METHODS

Cell Lines and Growth Conditions

All cell lines are derivatives of the Rat-1 cell line [Prouty et al., 1993] and were propagated as indicated [Mateyak et al., 1999]. For microscopic observation, cells were grown on glass cover slips. Sequences encoding either EYFP or three copies of the HA epitope (YPYDVPDYA) were placed directly in front of the initiator methionine residue of murine c-Myc using PCR and the tagged cDNA was cloned into the pLXSH retrovirus vector [Miller et al., 1993]. Virions were prepared by transfection of the BOSC23 packaging cell line [Pear et al., 1993] and used to infect HO15.19 (c-*myc*−/−) cells as described [Mateyak et al., 1999]. Following hygromycin selection, individual drug-resistant colonies were cloned with cloning rings and expanded in the absence of drug. HA-Myc clones were selected in 5 μg/ml blasticidin since they are in the pWZLblast backbone. For proteasome inhibition studies, cells were treated with 5 μM MG132 (Calbiochem, San Diego, CA) for 4 h at 37°C prior to fixation.

Cell Fixation

As described in detail elsewhere [Tam et al., 2002], coverslips were rinsed twice with Hanks balanced salt solution (HBSS) followed by ice-cold cytoskeletal buffer (CSK: 10 mM PIPES pH 6.8, 100 mM NaCl, 300 mM sucrose, 3 mM $MgCl_2$). Cells were then extracted for 3–5 min in ice-cold CSK containing 0.5% Triton X-100 (Roche, Indianapolis, IN) and 20 mM vanadyl ribonucleoside complex (Life Technologies, Rockville, MD), and subsequently fixed in 4% paraformaldehyde in Dulbecco's phosphate-buffered saline (PBS, pH 7.4) for 10 min at room temperature. Coverslips were stored in 70% ethanol at 4°C. Variations of this protocol as well as other protocols were tried, including fixation in paraformaldehyde followed by Triton permeabilization in CSK buffer, permeabilization by freeze-thawing [Kurz et al., 1996], or fixation in 100% cold methanol. We also tested whether storage of coverslips in PBS or 70% ethanol impacted the staining. In all cases staining was compared to c-*myc*−/− control cells treated identically.

Immunostaining

The following antibodies were used: goat anti-Daxx (Santa Cruz Biotechnology, Santa Cruz, CA, 1 μg/ml), rabbit anti-c-Myc (06-340) (Upstate Biotechnology, Lake Placid, NY, 10 μg/ml), rabbit anti-Myc N-262 (Santa Cruz), mouse anti-HA.11 (Covance, Inc., Princeton, NJ), rabbit anti-Max (Santa Cruz), mouse anti-mono- and poly-ubiquitinated protein (FK2) (Affiniti Research Products, Mamhead, UK), rabbit anti-PML (AB1370) (Chemicon, Temecula, CA). A second rabbit anti-PML, which worked well in rodent cells, was obtained from Paul Freemont (Imperial College of Science, Technology and Medicine, London) [Borden et al., 1995]. Cells were blocked with 1% bovine serum albumin in PBS (PBS–BSA), incubated with antibodies (diluted in PBS–BSA) for 1 h at 37°C, and washed successively (10 min each) in PBS, PBS with 0.1% Triton X-100, and PBS on a shaker. Rhodamine, AMCA or FITC-conjugated secondary antibodies, donkey anti-rabbit or donkey anti-goat (Jackson Immunoresearch, West Grove, PA) or AMCA, were diluted 1:500 in PBS–BSA and incubated with cells for 1 h at 37°C. Finally, coverslips were washed as indicated above and mounted with Vectashield (Vector Laboratories, Burlingame, CA).

Transient Transfection of EYFP-*myc*

Cells were grown on coverslips to a confluency of less than 50% and fed with fresh media 2 h prior to transfection. Cells were rinsed with serum-free, antibiotic free media before 0.5 μg of EYFP-*myc*, 2 μl of NovaFector (Venn Nova, Pompano Beach, FL) and 100 μl of serum-free, antibiotic free media was added to each coverslip. Coverslips were incubated for 1 h at 37°C before supplemented media was added to the cells. Coverslips were fixed anywhere from 2 to 24 h after the transfection.

Microscopic Analysis

Microscopy was done using Zeiss (Thornwood, NY) axioplan or Axiovert 200 microscopes with 100× plan-apo 1.4 objectives, triple band-pass filter sets (63000, Chroma, Brattleboro, VT), and a Z-axis motorized stage (LEP, Hawthorne, NY). Digital images were acquired by either a Photometrics (Tucson, AZ) Series 300 CCD, a Photometrics Quantix, or a Orca-ER (Hamamatsu, Bridgewater, NJ) camera. Image acquisition and analysis were done using Metamorph (Universal Imaging Corp., West Chester, PA) or Zeiss Axiovision 4.1 imaging software. Images shown are either single plane images of the best focal plane or, where noted, extended

focus images derived from z-stacks after constrained iterative deconvolution.

RESULTS

Characterization of HA-Myc Cell Lines

In clonal lines expressing an HA-tagged c-Myc transgene inserted into c-*myc*−/− fibroblasts (HO15.19), expression of the HA-Myc transgene completely reversed the characteristic enlarged morphology of the c-*myc*−/− cells (Fig. 1A). Proliferation rate measurements of exponentially growing cultures showed that the HA-Myc transgene effectively restored the slow growth phenotype of c-*myc*−/− cells to the growth rate of the parental cells (Fig. 1B). An important phenotype of c-*myc*−/− cells is a strong impairment of proliferation, which is accompanied by a significant reduction in S phase content of a population [Mateyak et al., 1997]. Flow cytometric analysis showed that HA-Myc completely restored the cell cycle DNA content profile to that of parental c-*myc*+/+ cells (Fig. 1C).

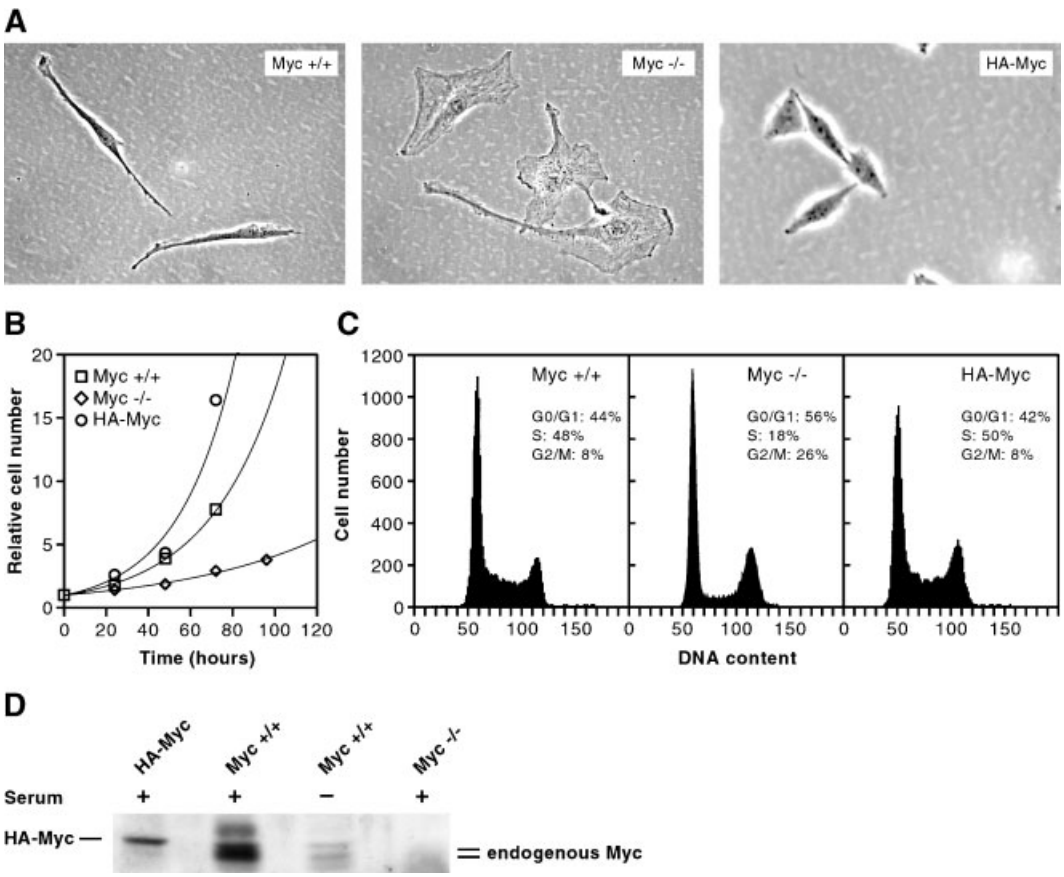

Fig. 1. Characterization of HA-Myc cells. **A**: Photomicrographs of actively growing cultures. Live cells growing on plastic were photographed with a Nikon Diaphot inverted microscope using a 40× objective and phase contrast optics. Images were captured with a CCD camera and processed in Adobe Photoshop. **B**: Cell proliferation curves. Exponentially growing cells were seeded at a density of 55,000 cells per 6-cm dish and exponentially growing cultures were harvested with trypsin at successive days and cell numbers were determined with a Coulter Counter. Each point represents the mean and standard deviations of (two) three plates per timepoint. (Exponential regressions of the data points were calculated and had R^2 values >0.95 in all cases.) **C**: DNA content measurements. Exponentially growing cultures were trypsinized, fixed with 70% ethanol, resuspended in PBS, and stained with 0.05 mg/ml propidium iodide as described previously [Shichiri et al., 1993]. DNA content was measured in a Becton Dickinson FACScan flow cytometer. **D**: Expression of endogenous c-Myc and HA-Myc transgene proteins. Cultures were grown to confluency, starved in 0.25% serum in DMEM for 48 h (−serum) followed by 4 h stimulation before harvesting with 10% serum in DMEM (+serum). Extracts (of cultures) were prepared in RIPA and 60 μg lysate was analyzed by SDS–PAGE, transferred to PVDF membrane and immunoblotted overnight at 4°C with 2 μg/ml anti c-Myc rabbit polyclonal antibody (Upstate Biotechnology, Lake Placid, NY, cat# 06-340) diluted in 3% milk-PBS. Primary antibody was detected with affinity purified goat-anti-rabbit-HRP (Jackson Immunoresearch, West Grove, PA, cat# 111035-144) diluted 1:8,000 in 3% milk-PBS–Tween-20 (0.075%) for 1 h at room temperature and the signal was visualized using Pico Western (Pierce, Rockford, IL) according to the manufacturers instructions.

To determine Myc protein expression levels, extracts of parental c-*myc*+/+ cells, c-*myc*−/− cells, and c-*myc*−/− cells expressing HA-Myc were immunoblotted with a polyclonal anti-Myc antibody (United Biomedical, Inc., Hauppauge, NY). The results clearly showed that HA-Myc was expressed at levels equivalent to or less than that of endogenous c-Myc in parental Rat-1 c-*myc*+/+ cells (Fig. 1D). The HA-Myc protein displayed a slightly reduced electrophoretic mobility due to the presence of the HA epitope tag.

This analysis was performed on three clonal cell lines recovered from the HA-Myc infection of c-*myc*−/− cells with very similar results. The data shown here were compiled from one cell line (clone 2) and are representative of the three cell lines. Clone 2 was chosen for further analysis because the expression level of HA-Myc was closest to that of endogenous Myc in Rat-1 cells; the other two clones showing higher levels.

In Situ Localization of c-Myc Protein

Several different fixation techniques were tested and the specificity of staining judged by comparison to two negative controls (TGR c-*myc*+/+ cells and *myc*−/− parental cells). There was very low background staining with the anti-HA antibody in *myc*−/− cells as compared to HA-*myc* cells (Fig. 2A). In cells expressing either the HA or EYFP tagged Myc proteins, we see a dispersed granular nucleoplasmic pattern that excludes the nucleoli (Fig. 2B–D). This dispersed pattern was seen in the majority of cells.

The use of *myc*−/− cells was particularly valuable in the assessment of staining with the endogenous anti-Myc antibodies, since prior studies had no way to judge background generated from the antibody versus detection of endogenous myc protein. The *myc*−/− control cells indicated that the antibodies to the endogenous protein displayed some non-specific signal that made them less reliable, particularly at low levels of Myc. This weak background fluorescence in *myc*−/− cells, when imaged, could generate the appearance of a finely "spotted" pattern, thus comparison to the *myc*−/− cells was an important negative control for evaluating endogenous antibody staining. We found the anti-Myc antibodies were more effective for detecting Myc when present at higher levels or concentrated in certain locales (see below). As shown in Figure 2B, the 06-340 anti-Myc antibody showed signal above background in cells that were more heavily labeled for EYFP-Myc, with essentially overlapping distribution of the two signals. Dual staining of HA-*myc* cells (Fig. 2C,D) with anti-HA and the anti-Myc antibodies (06-340 and N-262) shows a similar correlation. Note that intensity of anti-Myc staining matches that of anti-HA and EYFP in different nuclei.

Using three different detection methods and cells expressing Myc at approximately normal levels, our results indicate that typically c-Myc is distributed widely and more uniformly throughout the nucleoplasm. The Myc signal typically avoided (or was reduced in) the nucleolus. We found no evidence for c-Myc association with splicing factor rich SC-35 domains, as early observations with endogenous Myc antibodies had indicated [Sullivan et al., 1986; Spector et al., 1987]. Our consistent findings of a dispersed nucleoplasmic distribution for Myc are especially important in light of two recent reports that localized transiently-expressed, GFP-tagged Myc to a prominent nuclear spotted pattern (not overlapping SC35 domains) [Yin et al., 2001] versus a more uniform dispersed pattern [Arabi et al., 2003] (see Discussion).

Myc Proteins Accumulate in PML Bodies Upon Proteasome Inhibition of Rat Fibroblasts

Since Myc protein levels are regulated by the ubiquitin-proteasome pathway, we examined the relationship of Myc to PML bodies in cells treated with the proteasome inhibitor MG132. Cells were inhibited by the addition of 5 μM MG132 for 4 h. Although the distribution of tagged Myc appeared unaffected by the MG132 treatment in most cells (70%), proteasome inhibition produced HA-Myc and EYFP-Myc accumulations within PML bodies in ~20% of cells (Fig. 3A,B). While this pattern is observed in cells expressing tagged Myc at relatively normal levels, it is even more pronounced in cells in which EYFP-Myc is overexpressed by transient transfection (Fig. 3C). This effect was specific to PML bodies, as it was not seen for other nuclear bodies such as Cajal bodies or SC35 domains (not shown). Furthermore, other nuclear proteins, such as SC35 and coilin proteins (with or without GFP tags), were not seen to relocalize to PML bodies as HA and EYFP-Myc did. Although difficult to visualize above the background of the endogenous antibodies, in the parental rat fibroblast cell line TGR treated with MG132 endogenous Myc can

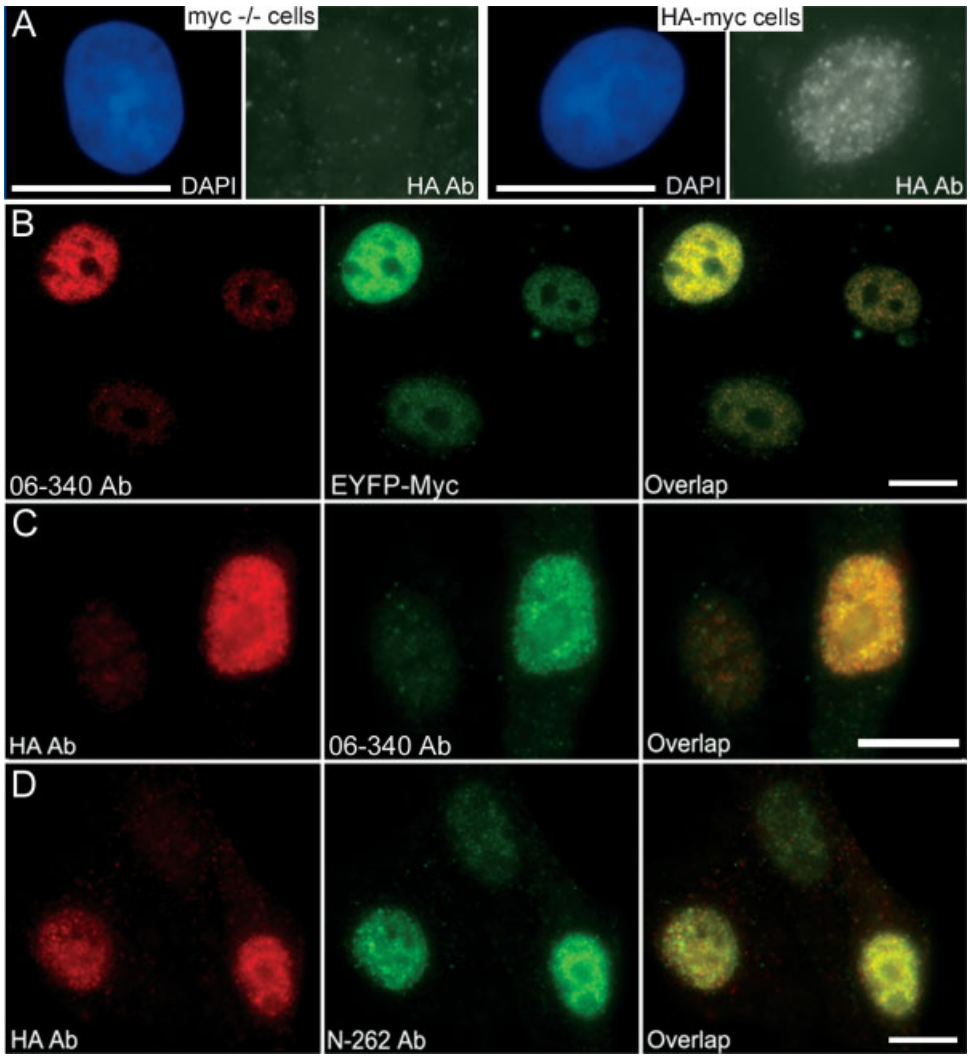

Fig. 2. Detection of Myc using a variety of techniques and antibodies shows a granular nucleoplasmic pattern. **A**: *myc*−/− and *myc*−/− cells stably transfected with HA-*myc* were stained with anti-HA antibody. Non-specific background staining in the *myc*−/− cells is very low compared to staining in the HA-Myc cells. **B**: Staining of EYFP-*myc* cells with the 06-340 anti-Myc antibody shows a granular nucleoplasmic pattern overlapping the GFP pattern. Staining of HA-*myc* cells with anti-HA antibody and the anti-Myc antibodies 06-340 (**C**) and N-262 (**D**) also show a granular pattern. Note that intensity of anti-Myc staining matches anti-HA and GFP intensities in different nuclei. Bar = 10 μm.

be seen in foci overlapping PML using the anti-Myc 06-340 antibody (Fig. 3D). The detection of the endogenous protein in cells carrying no modified Myc proteins supports that the accumulation of Myc in PML bodies is not due to the EYFP or HA tags. These experiments demonstrate that interference with Myc turnover by proteasome inhibition results in c-Myc accumulation within PML bodies.

Other observations further suggest a relationship between c-Myc and PML bodies. As seen in Figure 4A, in many cells transient overexpression of EYFP-Myc, in many cells, resulted in the formation of a very intensely stained aggregate that displaced chromatin as seen by DAPI staining. This result is similar to that reported previously for overexpressed c-Myc [Henriksson et al., 1988, 1992]. Strikingly, often PML bodies or accumulations of PML protein were found to redistribute to this large aggregation of Myc protein (Fig. 4D). In transiently transfected cells treated with MG132, the PML accumulation with Myc became even more pronounced, as did the large accumulations of Myc, likely due to impaired degradation of the EYFP-Myc. This effect was not seen for GFP-coilin or SC35 domains in MG132 treated cells (not shown), so it is not a result of a general

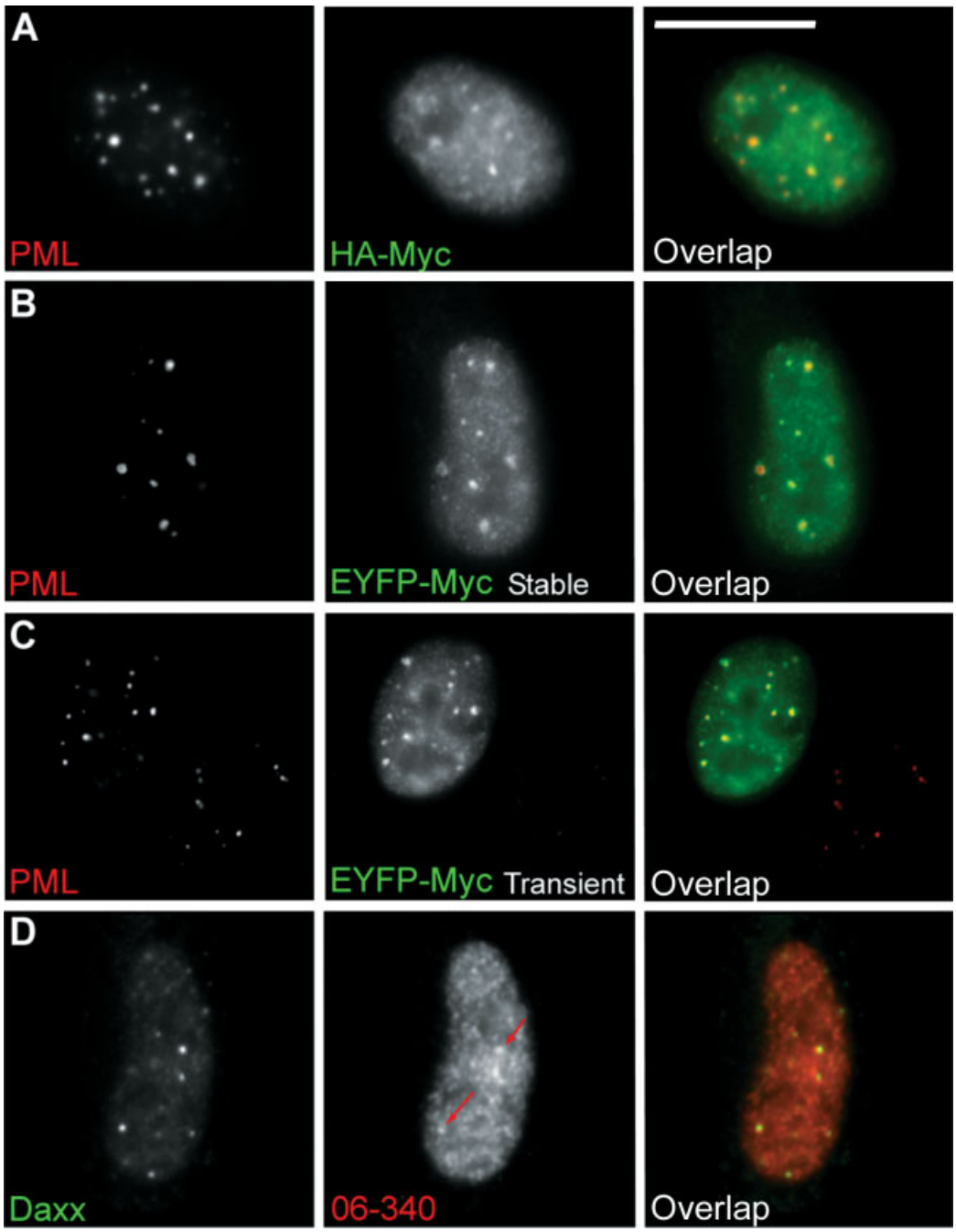

Fig. 3. The proteasome inhibitor MG132 causes tagged Myc protein to accumulate in PML bodies. Treatment with MG132 for 4 h frequently produces cells in which some HA-Myc (**A**, green) and EYFP-Myc (**B**, green) accumulate within PML bodies (red). **C**: Myc colocalization with PML bodies is more pronounced in cells in which EYFP-Myc is overexpressed by transient transfection. **D**: Faint foci of endogenous Myc detected with 06-340 anti-Myc (red, arrows) can be seen overlapping Daxx defined PML bodies (green). Bar = 10 μm.

aggregation of nuclear proteins. We do not suggest that this reflects the normal distribution of Myc protein; however the important point is that the PML protein/PML bodies show a clear affinity for these large accumulations of Myc protein. The images shown in Figure 4B–D suggest that as EYFP-Myc accumulations at individual PML bodies may increase until they eventually coalesce, ultimately drawing multiple intact PML bodies into a single large pool of Myc. While we consider these large singular accumulations of Myc protein to be an artifact of

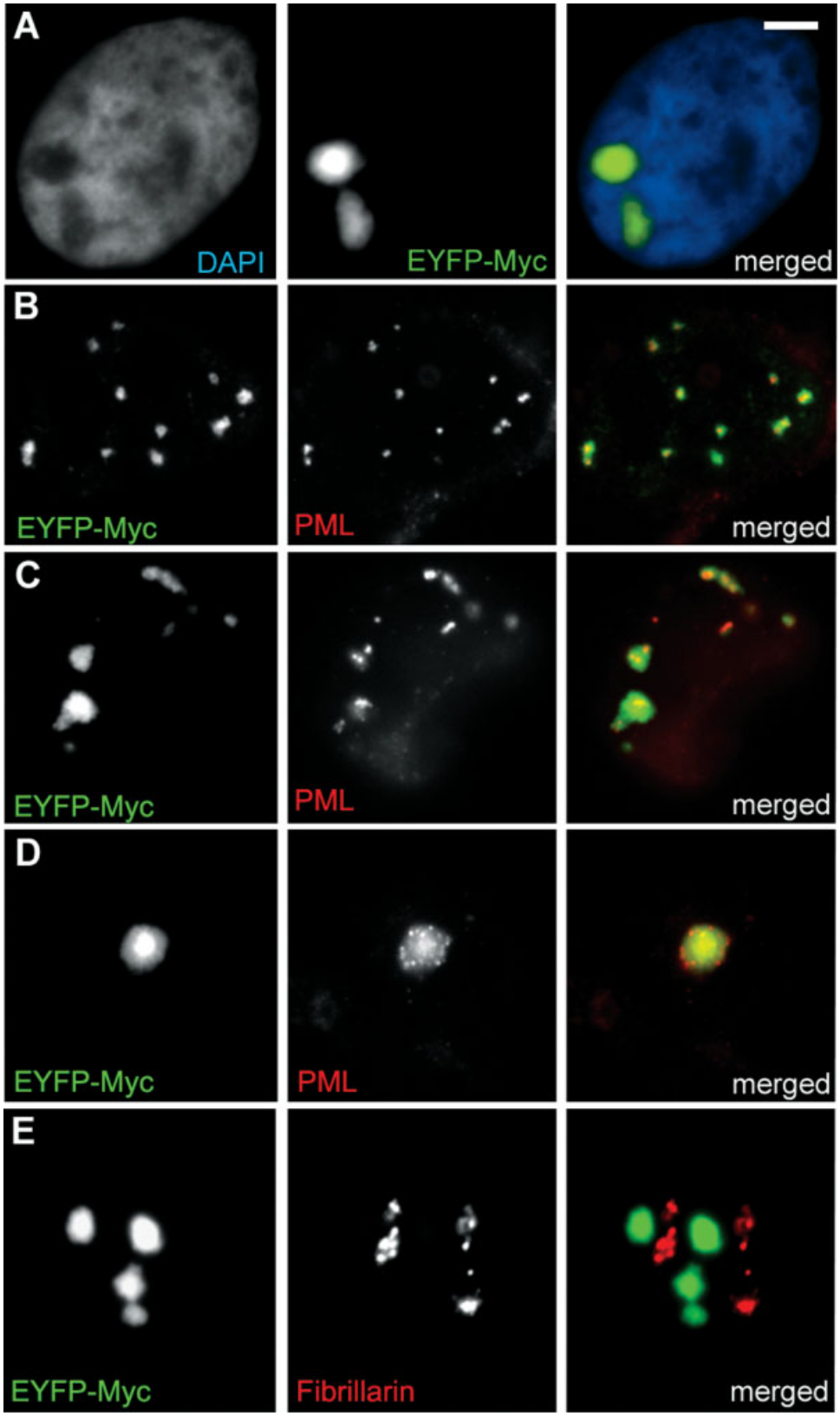

Fig. 4. Transiently overexpressed EYFP-Myc aggregates in large nuclear inclusions with PML. Transient transfection of TGR cells with EYFP-*myc* transgene produces some cells in which the EYFP-Myc protein is overexpressed and accumulates in large nuclear inclusions. This phenomenon is greatly enhanced by treatment with MG132 (seen here). **A**: Nuclear inclusions of EYFP-Myc (green) are in DAPI dark regions that could be mistaken for nucleoli. **B**: Association of EYFP-Myc (green) with PML bodies (red). **C**: Aggregation of PML (red) and EYFP-Myc (green). **D**: PML bodies (red) are all found within a large nuclear inclusion (green). **E**: Nuclear inclusions (green) are not associated with fibrillarin (red) and are not in nucleoli. Bar = 5 μm.

overexpression, the redistribution of PML bodies to these accumulations further supports some relationship between PML bodies and the Myc protein.

These large, very intense Myc aggregations seen under transient transfection conditions and proteasome inhibition did not correspond to the nucleolus as seen in Figure 4E. However, in addition to PML association, some cells did have increased nucleolar concentration of tagged Myc in the stable transfection lines, as addressed further below.

Distribution of Max and HA-Tagged Myc

Since Myc function requires its heterodimerization with Max, we next looked at the relative distributions of HA tagged Myc and endogenous Max using anti-HA and anti-Max antibodies. As shown in Figure 5A, both HA-Myc and Max have a granular appearance that is dispersed throughout the nucleus, excluding the nucleolus. Neither signal showed a clear or consistent overlap with Daxx defined PML bodies (Fig. 5A, inset). However, upon treatment with MG132, HA-Myc cells frequently have endogenous Max signals coincident with PML bodies (Fig. 5B) as seen for HA-Myc (Fig. 3).

Interestingly, staining of the *myc*−/− cells (HO15.19) for Max indicates that in some of these cells, small foci of Max are found with Daxx defined PML bodies in the absence of either Myc or proteasome inhibition (Fig. 5C). This accumulation was also seen less frequently in the normal parental fibroblasts (Fig. 5D). Although not seen in all cells, this result and the others described above suggests that Max and Myc associate with PML bodies. Further, they suggest that this association may be transient and potentially related to their turnover.

Myc and Max Distributions Relative to the Nucleolus

In addition to the pattern of Myc distributing with PML, MG132 treatment caused HA-Myc to accumulate in one or two large foci in about 20% of cells (Fig. 6A). While the very bright, large nuclear aggregates discussed above were not in the nucleolus, in some stably transfected cells

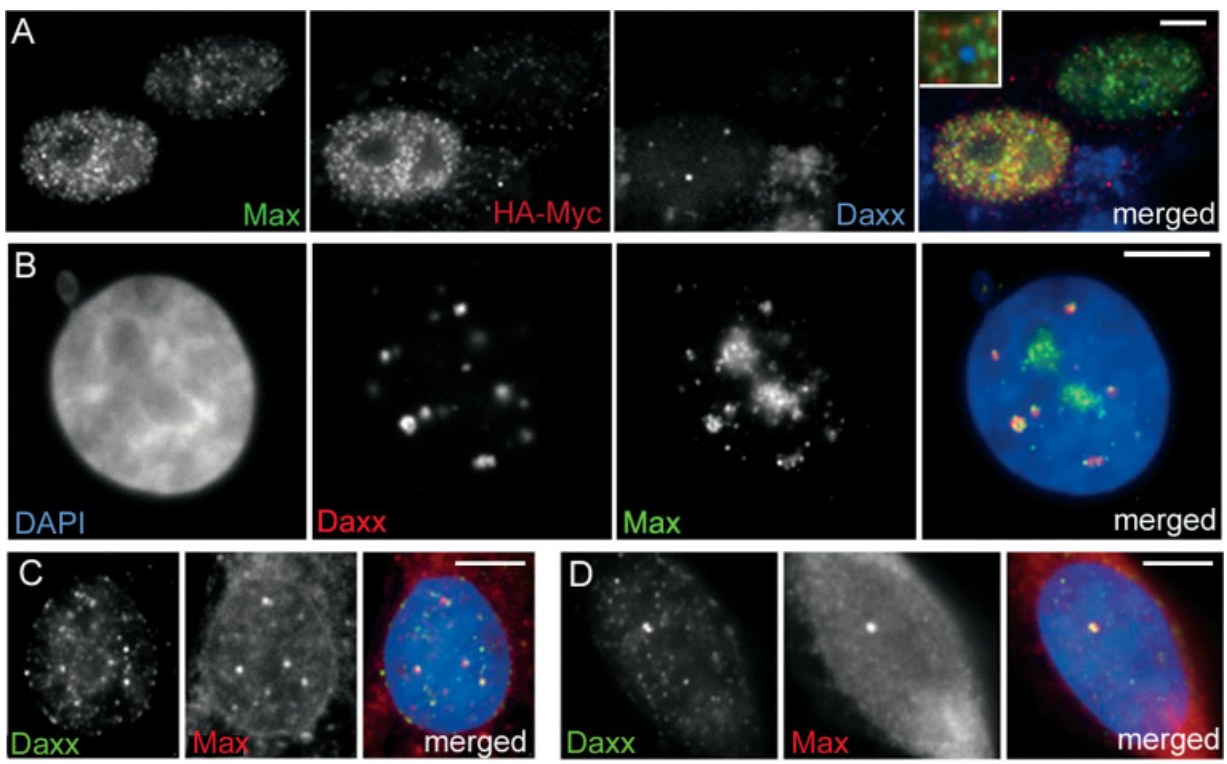

Fig. 5. Max distribution is similar to tagged Myc. **A**: An antibody to the Myc partner Max (green) shows a dispersed granular staining pattern that excludes the nucleolus, similar to HA-Myc (red). PML bodies (blue) do not have significant HA-Myc or Max staining (inset). **B**: Treatment of HA-Myc cells with the proteasome inhibitor MG132 causes Max (green) accumulation with Daxx defined PML bodies (red). Max foci (red) can often be found associated with PML bodies (green) in untreated *myc*−/− cells (**C**) and, less frequently, in TGR fibroblasts (**D**). Bar = 5 μm.

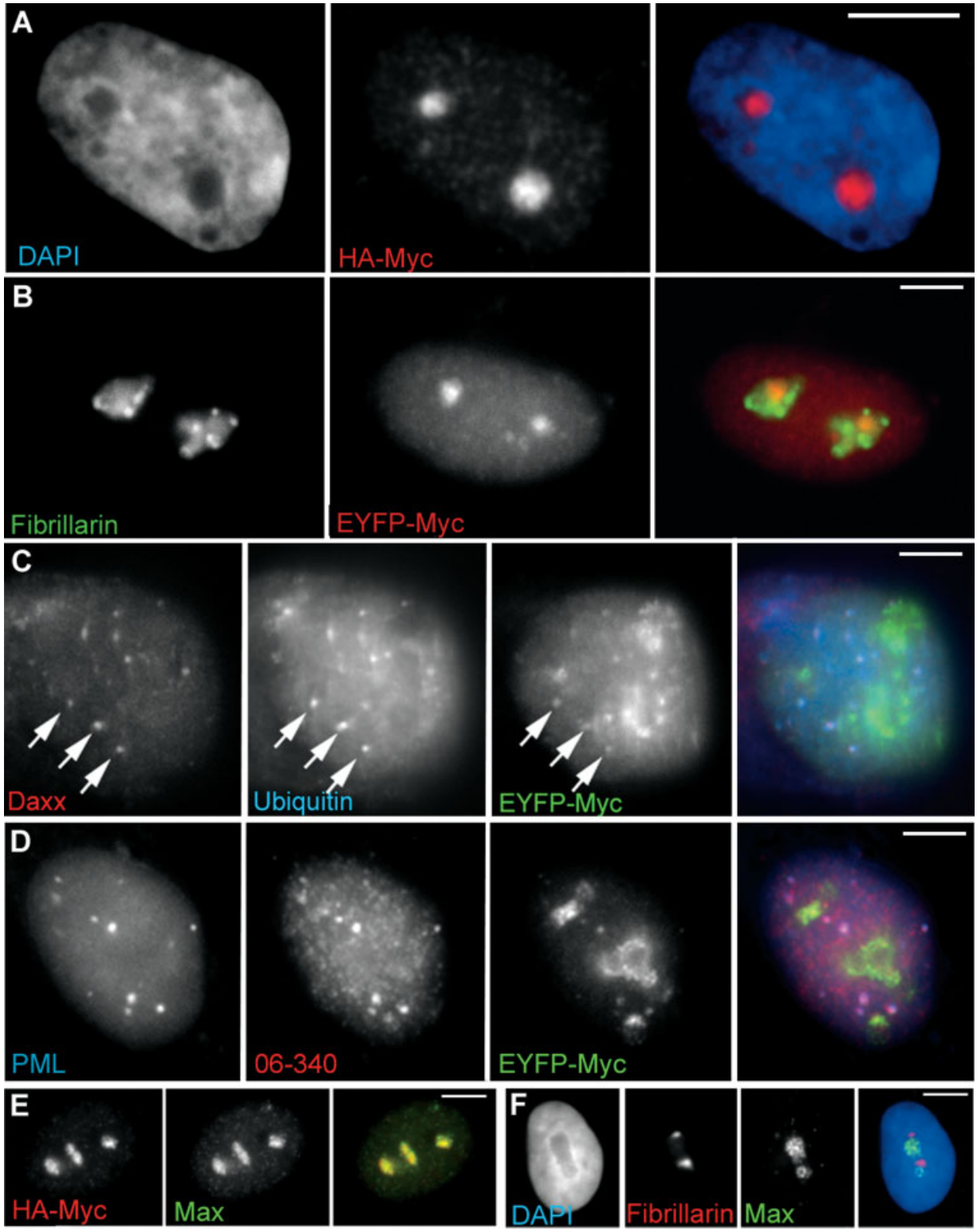

Fig. 6. Accumulations of Myc and Max can be found in the nucleolus in some MG132 treated cells. **A**: After MG132 treatment, HA-Myc (red) can be found accumulating in enlarged foci in some cells. DAPI staining (blue) suggests these foci are within nucleoli. **B**: Larger accumulations of EYFP-Myc (seen here as red) are associated with nucleoli detected by anti-fibrillarin (green). **C**: Ubiquitin (blue, arrows) is detected coincident with EYFP-Myc (green) and Daxx defined PML bodies (red), but not with the nucleolar accumulations of EYFP-Myc. **D**: The 06-340 anti-Myc antibody (red) detects foci overlapping PML bodies (blue) and EYFP-Myc spots (green), but does not detect the large EYFP-Myc accumulations in nucleoli. **E**: Max (green) colocalizes with HA-Myc (red) accumulations in some MG132 treated cells. **F**: As with Myc, these larger accumulations of Max (green) are adjacent to fibrillarin (red) in the nucleolus. Bar = 5 μm.

less intense but significant accumulations of Myc could be seen in DAPI weak regions corresponding to nucleoli. These foci, as seen with EYFP-Myc in Figure 6B, are adjacent to bright foci of fibrillarin, marking the nucleolar subcompartment referred to as the dense fibrillar component. The EYFP-Myc tends to form clusters abutting these brighter fibrillarin foci; hence, in some cells Myc appears to accumulate in a subcompartment of the nucleolus, excluding the dense fibrillar component, consistent with recently reported observations by Arabi et al. [2003].

Several observations indicate that the Myc protein localized to nucleoli in a subset of cells is distinct from that in the PML bodies. First, and most importantly, increased ubiquitin staining was coincident with the Myc protein in PML bodies, but not with the larger Myc accumulations found in the nucleolus (Fig. 6C). Since Myc is known to be ubiquitinated during turnover, this suggests that the nucleolus may not be a site of Myc degradation. Second, two observations suggest that the Myc protein in nucleoli is folded differently than in the rest of the cell. As shown in Figure 6D, EYFP-Myc concentrated in PML domains can be detected with an endogenous anti-Myc antibody. In contrast, the large accumulation of EYFP-Myc in the nucleolus was consistently undetectable with anti-Myc antibodies. This was not due to impenetrance of the nucleolus by antibodies, since fibrillarin and the HA tag were detected there (Fig. 6E,F), but appears to reflect a different folding which masks the endogenous epitope. Finally, observations on Max distribution suggest that the nucleolar accumulation of Myc may be a property of tagged Myc protein. The larger accumulations of Myc described above (Fig. 4) also contain significant amounts of Max (Fig. 6E) and appear to be in nucleoli by DAPI and fibrillarin staining (Fig. 6F). However, large Max accumulations were rare in MG132 treated TGR and *myc*−/− cells, suggesting that nucleolar accumulation may be a property of tagged Myc protein, perhaps due to misfolding in some cells.

Transfected Myc Accumulates With PML Bodies in HeLa Cells Without Proteasome Inhibition

To determine if Myc association with PML bodies could be reproduced in cells other than rat fibroblasts, we performed transient transfection of the human cervical carcinoma cell line HeLa with EYFP-tagged Myc. Transfected cells were either treated with proteasome inhibitor MG132 as described above, or left untreated. Approximately 50% of transfected, MG132 treated HeLa cells had EYFP-Myc foci overlapping PML nuclear bodies (not shown), indicating that Myc-PML body associations are not unique to rat fibroblasts. However, we were surprised to find that 28% of the transfected HeLa cells which were not treated with MG132 also had distinct EYFP-Myc foci overlapping PML body signals (Fig. 7). This colocalization occurred in nuclei where the EYFP-Myc was easily visible, but not highly overexpressed.

The transient expression of Myc in HeLa cells provides a key result of this study in that it shows that the accumulation of Myc with PML nuclear bodies is not exclusively a phenomenon of the TGR1 rat fibroblasts, but occurs in other species and cell types. Further, while the proteasome inhibition studies suggest a link between PML bodies and Myc turnover, the HeLa cell transfection also shows that this association is not merely a response due to exposure of the cells to the drug MG132, but reflects a bona fide relationship between c-Myc and PML bodies.

DISCUSSION

While two decades of research have made significant strides toward the elucidation of Myc regulation and function, a complete picture would be enhanced by resolution of the localization of Myc within the cell nucleus. Due to difficulties outlined in Introduction, this localization has been a point of contention for some time. In this study, reintroduction of EYFP or HA-tagged Myc by stable transfection into *myc* null cells has allowed the replacement of endogenous Myc with tagged Myc expressed at or near normal levels. Importantly, this tagged Myc is shown to functionally replace the endogenous Myc by the restoration of the normal cell morphology and growth rate. In these cells, the c-Myc protein is found throughout the nucleus in a dispersed granular pattern, as viewed by three methods. Most importantly, however, several observations provide the first evidence for a relationship of c-Myc and Max with PML bodies, and further point to the important possibility that the proteasome-mediated degradation of these factors occurs at the PML body.

The role of the PML body in degradation of endogenous proteins has been speculated recently [Anton et al., 1999; Reyes, 2001; Wojcik

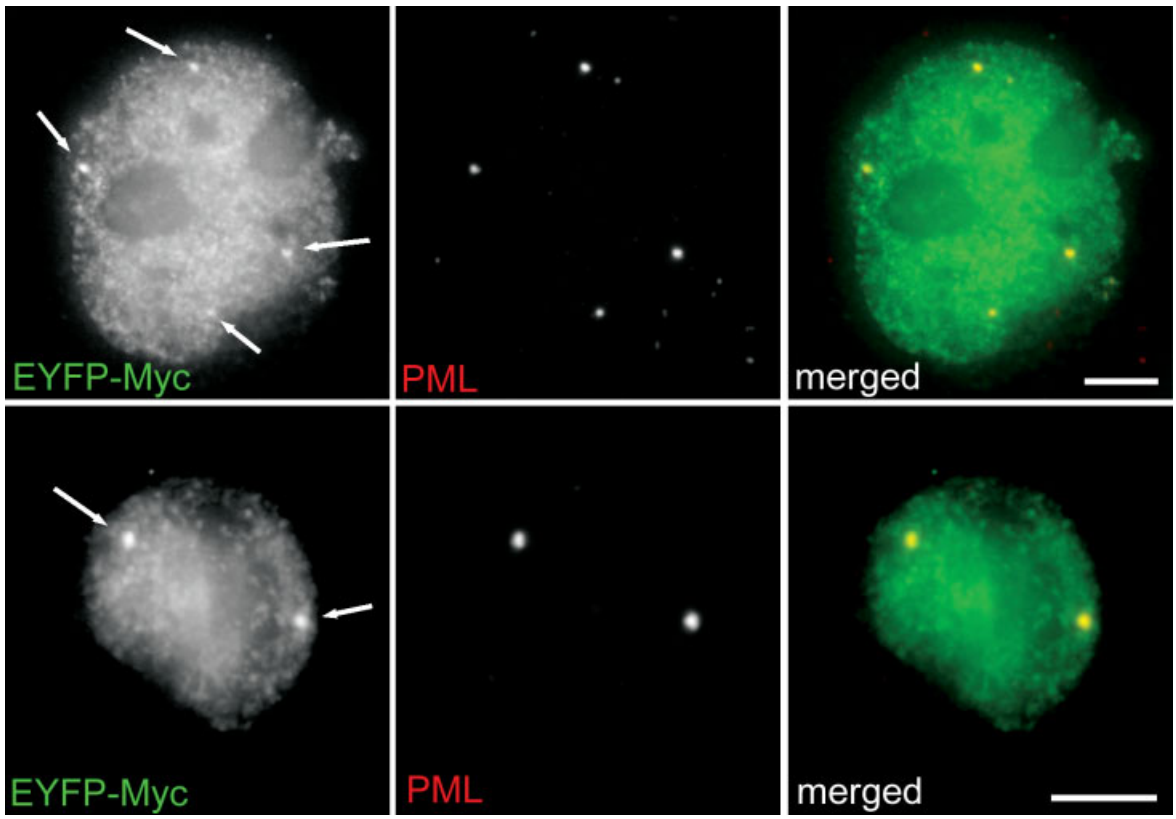

Fig. 7. EYFP-Myc transfected into HeLa cells accumulates at PML bodies without proteasome inhibition. Two examples of HeLa cell nuclei transiently transfected with EYFP-Myc (green) and stained with rabbit anti-PML antibody (AB1370) (red) showing overlap of Myc accumulations (arrows) with PML nuclear bodies without MG132 treatment. Shown are extended focus images derived from 100 nm z-stacks. Bar = 5 μm.

and DeMartino, 2003]. Our results fit well with other reports of the ubiquitin-mediated proteasomal degradation of Myc [Gross-Mesilaty et al., 1998; Salghetti et al., 1999; Sears et al., 1999] and the association of components of the 20S proteasomes [Fabunmi et al., 2001; Lallemand-Breitenbach et al., 2001] and ubiquitinated proteins [Anton et al., 1999; Everett, 2000] with PML bodies. It has also recently been shown that Myc exists in stable and unstable pools in the cell [Tworkowski et al., 2002]. We suggest that these pools could be made possible by differential localization; for example, short-lived Myc may localize to PML with stable Myc remaining in the nucleoplasm. The finding of endogenous Max association with PML bodies is also an important result, which supports a link between Myc/Max and PML bodies.

The disruption of PML bodies is a morphological hallmark of APL. Our results suggest the important possibility that if Myc turnover occurs at PML bodies, disruption of these structures in APL could hamper the normal degradation of Myc and possibly other oncoproteins. A recent publication [Dimberg et al., 2002] has shown that a primary event following treatment of APL cells with retinoic acid, known to cause APL remission and reformation of PML bodies, is down-regulation of c-Myc protein levels. Although, the authors treat this as down-regulation of Myc expression, we submit that reformation of PML bodies and a return to more normal Myc turnover could have reduced Myc levels. This prospect suggests that one potential mechanism of oncogenesis in APL could be misregulation of Myc turnover due to the disruption of their site of degradation, the PML body. We also note that most mutations in c-Myc that lead to cancer affect protein turnover. While many questions remain to be addressed, this study provides the first evidence for a potentially important link between PML bodies and Myc regulation. Unlike the rat fibroblasts cells, in HeLa carcinoma cells, GFP-Myc was readily evident within PML bodies in the absence of proteasome inhibition. Therefore, an

important prospect for future work will be to examine the extent to which cancer and non-cancer cells may differ in their distribution of Myc relative to PML bodies.

One goal of this study was to help clarify what has been a number of inconsistent observations concerning the intranuclear distribution of this important oncoprotein. While one early report of Myc localization described a dispersed granular appearance which may be consistent with our results [Hann et al., 1983], a later study reported that c-Myc colocalized with small nuclear ribonucleoprotein (snRNP) particles in nuclear speckles, also termed SC35 domains [Sullivan et al., 1986; Spector et al., 1987]. A recent paper investigated the localization of Myc and the Myc-interacting proteins Mad and Max by expression of transiently transfected GFP-tagged chimeric proteins [Yin et al., 2001]. The authors reported that Max produced a more diffuse nuclear staining whereas c-Myc and Mad localized in a number (~10–20) prominent nuclear spots, which did not overlap SC35 rich nuclear speckles. These spots may represent the same Myc accumulations at PML bodies we report here. Although, Yin et al. attempted to account for over-expression of Myc in their experiments, it is possible that the addition of transiently expressed tagged Myc cells already containing endogenous Myc may have resulted in a backlog of Myc degradation at the PML bodies, particularly in Cos-7 and 3T3 cells. Therefore, it would be of interest to see if the GFP-Myc foci seen in Yin et al. co-localize with PML bodies. While this manuscript was in preparation, another study appeared by Arabi et al. [2003] which independently also found that GFP-tagged Myc predominantly shows a dispersed nucleoplasmic distribution in transiently transfected cells. Thus our two studies are in agreement on this major point regarding transiently expressed Myc distribution in uninhibited fibroblasts. Although, we also saw some accumulation of c-Myc in the nucleolus in proteasome inhibited cells, our observations emphasized more the relationship of c-Myc to PML bodies, which was not noted by Arabi et al. On the other hand, they saw more pronounced staining of nucleoli in most cells after MG132 treatment, and emphasized the potential role of the nucleolus in Myc turnover. Several considerations may help to explain this difference. First, there is some overlap in the cytological observations, in that we did see association of Myc with the nucleolus to a lesser degree, and some images in Arabi et al. show nucleoplasmic spots that are consistent with PML body staining. Because Arabi et al. did not specifically co-stain for Myc and PML, the identity of these nucleoplasmic spots as PML bodies could easily have been missed. Second, there is clear evidence that under conditions of proteasome inhibition, PML body proteins relocate to the nucleolus, as shown in three different cell types examined [Mattsson et al., 2001]. Furthermore, MG132 treatment has been reported to cause nucleolar accumulation of endogenous p53 and MDM2 [Klibanov et al., 2001] as well as the EBV encoded EBNA-5 [Pokrovskaja et al., 2001], all of which localize to PML bodies under normal conditions. Thus, in Arabi et al., the inhibited Cos-7 or MCF-7 cells may well have had PML bodies and/or proteins redistributed to the nucleolus. In our rat fibroblast cells, we did not observe significant relocation of PML bodies to the nucleolus under the MG132 conditions tested, and therefore, may have been able to distinguish Myc localization to PML bodies versus the nucleolus, which would not be possible in cells where the two structures may merge. Our observation that ubiquitin staining overlapped PML bodies but not nucleoli after MG132 treatment further suggests that in our cells the PML bodies and not the nucleolus are more likely the site of Myc degradation. Interestingly, we show that in addition to the difference in ubiquitin, there is a difference in folding of Myc in the two compartments, evidenced by clear differences in the accessibility of the endogenous epitope.

ACKNOWLEDGMENTS

The Imaging Facility at Brown University was supported by the NIH grant RR-15578 from the COBRE Program of the National Center for Research Resources. The contents of this manuscript are solely the responsibility of the authors and do not necessarily represent the official views of the NIH.

REFERENCES

Abrams HD, Rohrschneider LR, Eisenman RN. 1982. Nuclear location of the putative transforming protein of avian myelocytomatosis virus. Cell 29:427–439.

Amati B, Frank SR, Donjerkovic D, Taubert S. 2001. Function of the c-Myc oncoprotein in chromatin remodeling and transcription. Biochim Biophys Acta 1471: M135–M145.

Anton LC, Schubert U, Bacik I, Princiotta MF, Wearsch PA, Gibbs J, Day PM, Realini C, Rechsteiner MC, Bennink JR, Yewdell JW. 1999. Intracellular localization of proteasomal degradation of a viral antigen. J Cell Biol 146:113–124.

Arabi A, Rustum C, Hallberg E, Wright AP. 2003. Accumulation of c-Myc and proteasomes at the nucleoli of cells containing elevated c-Myc protein levels. J Cell Sci 116:1707–1717.

Ascoli CA, Maul GG. 1991. Identification of a novel nuclear domain. J Cell Biol 112:785–795.

Baudino TA, Cleveland JL. 2001. The Max network gone mad. Mol Cell Biol 21:691–702.

Borden KL, Boddy MN, Lally J, O'Reilly NJ, Martin S, Howe K, Solomon E, Freemont PS. 1995. The solution structure of the RING finger domain from the acute promyelocytic leukaemia proto-oncoprotein PML. EMBO J 14:1532–1541.

Claassen GF, Hann SR. 1999. Myc-mediated transformation: The repression connection. Oncogene 18:2925–2933.

Cole MD, McMahon SB. 1999. The Myc oncoprotein: A critical evaluation of transactivation and target gene regulation. Oncogene 18:2916–2924.

Darzacq X, Jady BE, Verheggen C, Kiss AM, Bertrand E, Kiss T. 2002. Cajal body-specific small nuclear RNAs: A novel class of 2′-*O*-methylation and pseudouridylation guide RNAs. EMBO J 21:2746–2756.

Dimberg A, Bahram F, Karlberg I, Larsson LG, Nilsson K, Oberg F. 2002. Retinoic acid-induced cell cycle arrest of human myeloid cell lines is associated with sequential down-regulation of c-Myc and cyclin E and posttranscriptional up-regulation of p27(Kip1). Blood 99:2199–2206.

Dyck JA, Maul GG, Miller J, Miller WH, Chen JD, Kakikuza A, Evans RM. 1994. A novel macromolecular structure is a target of the promyelocyte-retinoic acid receptor oncoprotein. Cell 76:333–343.

Everett RD. 2000. ICP0 induces the accumulation of colocalizing conjugated ubiquitin. J Virol 74:9994–10005.

Everett RD, Meredith M, Orr A, Cross A, Kathoria M, Parkinson J. 1997. A novel ubiquitin-specific protease is dynamically associated with the PML nuclear domain and binds to a herpesvirus regulatory protein. EMBO J 16:1519–1530.

Fabunmi RP, Wigley WC, Thomas PJ, DeMartino GN. 2001. Interferon gamma regulates accumulation of the proteasome activator PA28 and immunoproteasomes at nuclear PML bodies. J Cell Sci 114:29–36.

Gall JG. 2000. Cajal bodies: The first 100 years. Annu Rev Cell Dev Biol 16:273–300.

Gross-Mesilaty S, Reinstein E, Bercovich B, Tobias KE, Schwartz AL, Kahana C, Ciechanover A. 1998. Basal and human papillomavirus E6 oncoprotein-induced degradation of Myc proteins by the ubiquitin pathway. Proc Natl Acad Sci USA 95:8058–8063.

Hann SR, Abrams HD, Rohrschneider LR, Eisenman RN. 1983. Proteins encoded by v-*myc* and c-*myc* oncogenes: Identification and localization in acute leukemia virus transformants and bursal lymphoma cell lines. Cell 34: 789–798.

Henriksson M, Classon M, Axelson H, Klein G, Thyberg J. 1992. Nuclear colocalization of c-myc protein and hsp70 in cells transfected with human wild-type and mutant c-*myc* genes. Exp Cell Res 203:383–394.

Henriksson M, Classon M, Ingvarsson S, Koskinen P, Sumegi J, Klein G, Thyberg J. 1988. Elevated expression of c-*myc* and N-*myc* produces distinct changes in nuclear fine structure and chromatin organization. Oncogene 3: 587–593.

Henriksson M, Luscher B. 1996. Proteins of the Myc network: Essential regulators of cell growth and differentiation. Adv Cancer Res 68:109–182.

Hershko A, Ciechanover A. 1998. The ubiquitin system. Annu Rev Biochem 67:425–479.

Klibanov SA, O'Hagan HM, Ljungman M. 2001. Accumulation of soluble and nucleolar-associated p53 proteins following cellular stress. J Cell Sci 114:1867–1873.

Kretzner L, Blackwood EM, Eisenman RN. 1992. Myc and Max proteins possess distinct transcriptional activities. Nature 359:426–429.

Kurz A, Lampel S, Nickolencko JE, Bradl J, Benner A, Zirbel RM, Lichter P. 1996. Active and inactive genes localize to the periphery of chromosome territories. J Cell Biol 135:1195–1205.

Lallemand-Breitenbach V, Zhu J, Puvion F, Koken M, Honore N, Doubeikovsky A, Duprez E, Pandolfi PP, Puvion E, Freemont P, de The H. 2001. Role of promyelocytic leukemia (PML) sumolation in nuclear body formation, 11S proteasome recruitment, and As2O3-induced PML or PML/retinoic acid receptor alpha degradation. J Exp Med 193:1361–1371.

Lamond AI, Earnshaw WC. 1998. Structure and function in the nucleus. Science 280:547.

Mateyak MK, Obaya AJ, Adachi S, Sedivy JM. 1997. Phenotypes of c-Myc-deficient rat fibroblasts isolated by targeted homologous recombination. Cell Growth Differ 8:1039–1048.

Mateyak MK, Obaya AJ, Sedivy JM. 1999. c-Myc regulates cyclin D-Cdk4 and -Cdk6 activity but affects cell cycle progression at multiple independent points. Mol Cell Biol 19:4672–4683.

Mattsson K, Pokrovskaja K, Kiss C, Klein G, Szekely L. 2001. Proteins associated with the promyelocytic leukemia gene product (PML)-containing nuclear body move to the nucleolus upon inhibition of proteasome-dependent protein degradation. Proc Natl Acad Sci USA 98:1012–1017.

Miller AD, Miller DG, Garcia JV, Lynch CM. 1993. Use of retroviral vectors for gene transfer and expression. Methods Enzymol 217:581–599.

Moen PT, Smith KP, Lawrence JB. 1995. Compartmentalization of specific pre-mRNA metabolism: An emerging view. Hum Mol Genet 4:1779–1789.

Pear WS, Nolan GP, Scott ML, Baltimore D. 1993. Production of high-titer helper-free retroviruses by transient transfection. Proc Natl Acad Sci USA 90:8392–8396.

Pokrovskaja K, Mattsson K, Kashuba E, Klein G, Szekely L. 2001. Proteasome inhibitor induces nucleolar translocation of Epstein–Barr virus-encoded EBNA-5. J Gen Virol 82:345–358.

Prouty SM, Hanson KD, Boyle AL, Brown JR, Shichiri M, Follansbee MR, Kang W, Sedivy JM. 1993. A cell culture model system for genetic analyses of the cell cycle by targeted homologous recombination. Oncogene 8:899–907.

Ramsay G, Stanton L, Schwab M, Bishop JM. 1986. Human proto-oncogene N-*myc* encodes nuclear proteins that bind DNA. Mol Cell Biol 6:4450–4457.

Reyes JC. 2001. PML and COP1—two proteins with much in common. Trends Biochem Sci 26:18–20.

Salghetti SE, Kim SY, Tansey WP. 1999. Destruction of Myc by ubiquitin-mediated proteolysis: Cancer-associated and transforming mutations stabilize Myc. EMBO J 18:717–726.

Salomoni P, Pandolfi PP. 2002. The role of PML in tumor suppression. Cell 108:165–170.

Sears R, Leone G, DeGregori J, Nevins JR. 1999. Ras enhances Myc protein stability. Mol Cell 3:169–179.

Shichiri M, Hanson KD, Sedivy JM. 1993. Effects of c-*myc* expression on proliferation, quiescence, and the G_0 to G_1 transition in nontransformed cells. Cell Growth Differ 4: 93–104.

Shopland LS, Lawrence JB. 2000. Seeking common ground in nuclear complexity [comment]. J Cell Biol 150:F1–F4.

Spector DL, Watt RA, Sullivan NF. 1987. The v- and c-*myc* oncogene proteins colocalize in situ with small nuclear ribonucleoprotein particles. Oncogene 1:5–12.

Sullivan NF, Watt RA, Delannoy MR, Green CL, Spector DL. 1986. Colocalization of the myc oncogene protein and small nuclear ribonucleoprotein particles. Cold Spring Harb Symp Quant Biol 51:943–947.

Tam R, Johnson C, Shopland L, McNeil J, Lawrence JB. 2002. Applications of RNA FISH for visualizing gene expression and nuclear architecture. In: Beatty B, Mai S, Squire J, editors. FISH. Oxford: Oxford University Press. p 93–118.

Tworkowski KA, Salghetti SE, Tansey WP. 2002. Stable and unstable pools of Myc protein exist in human cells. Oncogene 21:8515–8520.

Waters CM, Littlewood TD, Hancock DC, Moore JP, Evan GI. 1991. c-myc protein expression in untransformed fibroblasts. Oncogene 6:797–805.

Weis K, Rambaud S, Lavau C, Jansen J, Carvalho T, Carmo-Fonseca M, Lamond A, Dejean A. 1994. Retinoic acid regulates aberrant nuclear localization of PML-RARalpha in acute promyelocytic leukemia cells. Cell 76:345–356.

Wojcik C, DeMartino GN. 2003. Intracellular localization of proteasomes. Int J Biochem Cell Biol 35:579–589.

Yin X, Landay MF, Han W, Levitan ES, Watkins SC, Levenson RM, Farkas DL, Prochownik EV. 2001. Dynamic in vivo interactions among Myc network members. Oncogene 20:4650–4664.

Zhong S, Salomoni P, Pandolfi PP. 2000. The transcriptional role of PML and the nuclear body. Nat Cell Biol 2: E85–E90.